Structural Features of Cholinium Based Protic Ionic Liquids Through Molecular Dynamics.

Andrea Le Donne[a], Henry Adenusi[a], Francesco Porcelli[a], Enrico Bodo[a1]

[a] *Chemistry Department, University of Rome "La Sapienza", Piazzale Aldo Moro 5, 00185, Rome Italy*

ABSTRACT

An analysis of the complex proton transfer processes in certain protic ionic liquids, based on amino acid anions, has been carried out through ab-initio molecular dynamics in the view of finding naturally conductive and pure mediums. The systems analysed here might serve as chemical prototypes for pure and dry ionic liquids where mobile protons can act as fast charge carriers. We have exploited the natural tendency of these liquids to form a complex network of hydrogen bonds. The presence of such network allows the naturally repulsive interaction between like charge ions to be weakened to the point that proton migration process inside the anionic component of the fluid becomes possible. We have also seen that the extent of this proton migrations is sizable for carboxylic based amino acid anions while is very limited for sulphur containing ones.

1. Introduction

The developing field of ionic liquids (ILs) is home to a class of materials known as protic ionic liquids (PILs) which have received increased interest due to their remarkable physicochemical properties [1,2,3]. It has been proven possible to synthetize ILs made exclusively of bio-organic species whose affinity for biological molecules could open new routes in pharmaceutical applications [4].

Most PILs, as other ILs, possess low volatility, thermal stability, and versatility enabling them for use in industrial settings such as electrolytes in batteries and supercapacitors. A key benefit of PILs might stem from their anhydrous proton conductivity. Further investigation of the ionic transport behaviour of these materials is essential for the design of electrochemical devices with improved performance and safety.

PILs are generally synthesized using equimolar amounts of Brönsted acid and a Brönsted base where a proton transfer from the acid to the base leads to ionization and to the ensuing formation of proton donor/acceptor sites that spawn a hydrogen bonding network. Typically, the degree of ionization in a PIL is dependent on the ΔpKa between the acid and conjugate acid of the base. It is understood that a large difference in the pKa's of the reagents (>6) ensures the resulting liquid is substantially fully

[1] Corresponding Author. Email: enrico.bodo@uniroma1.it

ionized [5]. When the difference in pKa is small, a certain fraction of the molecular constituents remains neutral, hence causing a partial loss of the IL properties, phase separations and evaporation [6].

Beyond the electrochemical implications, PILs are gaining further attention because they display multifaceted interactions as well as intriguing chemical activity, intricate phenomena and complex hydrogen bonding features [7,8,9,10,11].

Moreover, it is evident that the nanoscopic structure of their molecular constituents impacts the properties and thus the function of the bulk state of these compounds especially if secondary protic functional groups are present in the structure [12]. The rationale of this lies in the fact that the range of the possible cation (base) and anion (acid) combinations for PILs is so large, that the physicochemical properties of these liquids can, in principle, be tuned for task specific purposes. In particular, suitable chemical modifications of the molecular constituents should permit the rational modulation of the bulk liquid properties, a feature that has led to investment of task-specific ILs in many fields [13].

Herein we investigate an homologue series of compounds made up of a singly deprotonated amino acid anion (AA), from now on $[AA]^-$, which represents the variable (tunable) part of the fluid, and a choline cation, from now on $[Ch]^+$, which is, instead, the same for all liquids. The pKa difference between a typical COOH in the amino acid and the choline cation is around 11 units. Therefore, an ionic liquid made by choline and a deprotonated amino acid is a fully ionic system with very little or no neutral components. The AAs we are going to analyse in this work, possess another protic function on the side chain that provides an additional degree of freedom in terms of proton equilibria and that, in turn, makes these compounds extremely interesting as a realistic model for conducting, anhydrous, highly ionized media. The AAs which are the focus of this study are: aspartic acid $[Asp]^-$, glutamic acid $[Glu]^-$, cysteine $[Cys]^-$, and homocysteine $[HCys]^-$.

These compounds have been synthesized [14], turn out to be fully biocompatible [15,16] and non-toxic to humans as well as to the environment, since the constituents are both involved in metabolic processes [17]. As a result, this class of materials have potential for use in biomedical and medicinal research [18,19,20,21]. Furthermore, their possible dry proton conductivity makes them prospective candidates in electrochemistry [22,23,24,25,26,27,28,29].

In this work, we explore the nanoscopic structure of these systems utilising both ab-initio computations and molecular dynamic simulations. In addition to the presence of a very complex hydrogen bonding network, the compounds we examine here can sustain a proton migration process via intra and inter-molecular transfers. The latter has been observed in previous theoretical studies [30] [31] [32] and is made possible because of the presence of a mobile proton on the (non-deprotonated) side chain. The migration of this proton occurs through two different mechanisms that involve either an intra- or an inter-molecular transfer. The proton transfer generates a peculiar and transient chemical

structure with a "three-charge" separation (see Scheme 1, upper right structure) that is an anionic equivalent of the amino acid zwitterionic structures (we indicate these structures with the acronym ZWA – zwitterionic anion).

The first negative charge on the AA is located on the most acidic carboxylate group and it appears due to the primary deprotonation process which is implicit in the combination with the choline base, that, formally, can be written as:

$HR–CH(NH_2)–COOH + Ch \rightarrow HR–CH(NH_2)–COO^- + [Ch]^+$

where Ch is a shorthand for a deprotonated cholinium base and HR– represents the acidic side chain on $[AA]^-$.

The second and third charges are generated when the proton transfers from the side chain to the amino group which becomes positively charged. This happens both in the same molecule (an intramolecular proton transfer or tautomerization process):

$HR\text{-}CH(NH_2)–CO_2^- \rightarrow {}^-R–CH\ (NH_3)^+–CO_2^-$ (1)

or between different anions through a complex sequence of proton transfers that can be summarized as:

$HR\text{-}CH(NH_2)–CO_2^- + HR\text{-}CH(NH_2)–CO_2^- \rightarrow {}^-R–CH(NH_3)^+–CO_2^- + {}^-R\text{-}CH(NH_3)^+–CO_2^-$ (2)

Both reactions (1) and (2), for clarity, have also been drawn in Scheme 1.

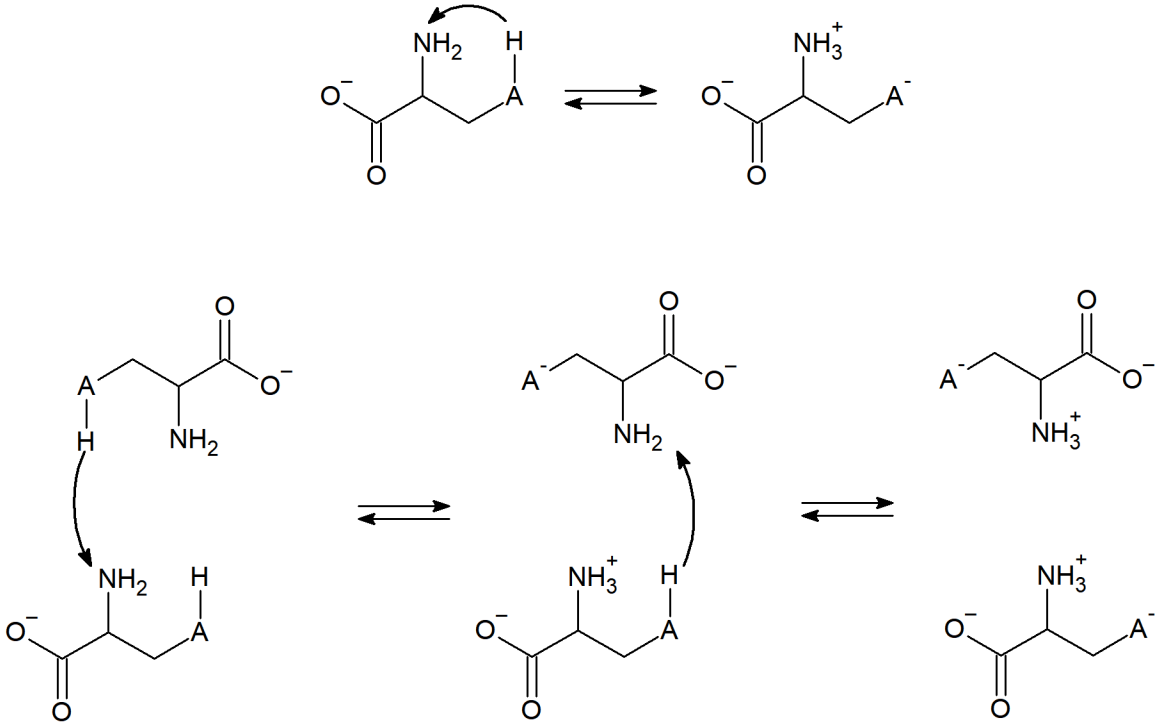

Scheme 1: Intramolecular (top) and intermolecular (bottom) proton transfer between anions.

Hence, in the liquid we have a single chemical specie for the cation $[Ch]^+$ and two possible isomeric forms of the AA. The first one is a simple anionic form with a carboxylate as in the reactants of

reaction (1) and (2), the second is a zwitterionic anion (ZWA) as those formed in reactions (1) and (2).

While the formation of ZWA, in principle, can take place by intra-molecular proton transfer, we have recently shown [9] [10] that it is actually more likely to occur between two different anions. In order to occur in the liquid, this kind of proton transfer, requires two anions to be sufficiently close. One of the counterintuitive features of PIL, and of these compounds in particular, is that the anionic species can cluster together to form like-charge dimers and trimers through strong hydrogen bonds [33]. A similar behaviour has been also noticed in other PIL, but between the cationic moieties [30] [34] [35] [36]. We also point out that such unconventional ZWA tautomers have been identified experimentally for $[Cys]^-$ proving that they exist under certain conditions [37].

Analysis of previous MD simulations [33] supported the existence of these unusual ZWA species in the bulk liquid in the amino acids such as $[Asp]^-$ and $[Cys]^-$ where we have the necessary acidic functionality in their side chain. The existence of ZWA is a unique feature of these compounds and contradicts the common assumption which sees ILs as constituted by an alternating pattern of charges. It is our belief that the presence of ZWA species can impact the bulk properties of these already complex systems. Their formation is particularly intriguing because the degree of anionic association seems to be in a direct relation with bulk properties such as viscosity and melting temperatures [33]. As we have previously shown, [33] aliphatic AAs show a weaker tendency to cluster together, precisely because they lack an extra acidic function.

The extent of the proton transfer process (2) and the relative abundances of the two isomeric forms of the AAs are the subject of this work in the view of providing a template of a dry ionic liquid with high proton mobility. In other words, the aim of this work is to comprehend the structural complexity of these zwitterionic species, to understand their occurrence in the bulk phase of PILs and to explore the possibility that their formation may provide a chemical channel to fast, dry proton conduction.

2. Computational Methods

Preliminary, ab-initio calculations have been carried out both on the cation-anion dimers (made by a deprotonated $[AA]^-$ plus a choline cation $[Ch]^+$) and dimers made by two AAs. The 4 different dimer combinations that have been studied are: [Ch][AA], [Ch][ZWA], $[AA_2]^{2-}$ and $[ZWA_2]^{2-}$. We have limited the calculation to 4 AA, namely: $[Asp]^-$, $[Glu]^-$, $[Cys]^-$ and $[HCys]^-$. Given that chemical species with charge separations are highly unstable in vacuum and in order to make our models more realistic, we have included an environmental dielectric screening. All the ab-initio calculations have been therefore performed in a continuum solvent model (PCM). While, the dielectric permittivity of these compound has yet to be stated in the literature, we have used the acetonitrile PCM parameters

as a realistic model solvent as its dielectric constant (ε=35.7) matches the typical value of other PILs [38,39]. For each structure, we have performed a fully unconstrained optimization and evaluated the harmonic frequencies using D3-B3LYP [40] with the 6-311+G** basis set. This functional is suitable for such a study since it provides results that are comparable to the more accurate D3-B2PLYP functional, as was verified in one of our recent studies [33]. The Gaussian16 [41] package was utilised for the ab-initio calculations.

The study of the bulk phase of the 4 AA-based ionic liquids has been achieved by ab-initio molecular dynamics (AIMD), which has the advantage of computing the "exact" nuclear forces from the electronic structure without the use of a *fixed chemical topology* and the inevitable approximations that characterize the force field-based methods. Although reactive force fields do exist, their applicability to the study of protic equilibria in ionic liquid has not yet been implemented. Therefore, the only way to approach to the study of proton transfer processes in ionic liquids, at the moment, is represented by semiempirical and ab-initio methods that are based on the evaluation of the atomic forces from an approximate solution of the electronic Schrodinger equation. The former however suffers from a lack of applicability in this specific case because their parametrization is heavily dependent upon the chosen training set. Although, following the above argument, ab-initio molecular dynamics certainly provides a robust choice for this study, it suffers from two main pitfalls: (i) the resulting computations are very demanding so that the time-span of the simulations is limited to few tens of ps; and (ii) the size of the systems that can be treated using this approach is limited. In this regard we point out that, due to these intrinsic limits, our computations cannot provide a reliable thermodynamical model of the fluid at equilibrium (which would require to simulate times of the order of ns). Nevertheless, what we can grasp from our simulations are the local structural features of the bulk fluid and the fundamental molecular processes that drive the proton diffusion that, at equilibrium, would ultimately characterize the fluid state.

Different aspects of the simulations pertaining to the [Ch][Asp] and [Ch][Cys] systems have been already discussed by us previously [9,10] and we defer the reader to these papers for the computational details. The bulk simulations of the [Ch][HCys] and [Ch][Glu] systems are presented here for the first time and have been performed with Car-Parinello molecular dynamics and the CPMD code [42] using a cell with a side length of around 20 Å filled with 24 ionic pairs. CPMD has been performed employing Troullier-Martins pseudopotentials and the BLYP functional. The production time is 39 ps at 360 K in the NVT ensemble. A complete list of all simulation parameters of all systems is reported inside the Supporting Information (SI).

3. Results and Discussion

In this series of homologous PILs it is understood that the anion structure influences the bulk properties of the liquid such as viscosities, melting points and, to a lesser extent, density. This is rather obvious since the AA anion contains, on the side chain, the "tuneable" moiety in the fluid which is, in turn, responsible for the complexity of the local structure. The presence of the additional proton gives rise to proton transfer equilibria and tautomerization reactions. Such reactions provide a source of ZWAs in the liquid, thereby locally altering the charge distribution.

We begin our analysis by presenting the association enthalpies for the various ionic couples that can be formed in the liquid, all calculated in the presence of a dielectric medium (PCM). The data are reported in Table 1 where we present the association energies of the [Ch][AA], [Ch][ZWA], $[AA_2]^{2-}$ and $[ZWA_2]^{2-}$ dimers. All the dimers turned out to be stable with respect to the isolated fragments despite the fact that some of them ($[AA_2]^{2-}$ and $[ZWA_2]^{2-}$) are made by like-charge ions that present a repulsive electrostatic interaction. The stabilisation of these dimers is due to hydrogen bonding interactions which is dependent on the type of side chain present in the amino acid anion. A comparison of these interaction energies allows us to trace the relative stability of the binary structures that can appear in the liquid phase so to help the interpretation of the bulk phase data which, as we shall see, are rather complicated. The optimized structures for a selected set of $[AA_2]^{2-}$ and $[ZWA_2]^{2-}$ dimers are reported in Figures 1-3. All the other structures are reported in Figure S2-S5 in the supporting information.

Table 1: B3LYP-D3/6-311+G (PCM with ε=35.7) ΔH° of the different dimer association in kcal/mol.**

	[Ch][AA]	**[Ch][ZWA]** [a]	**$[AA_2]^{2-}$**	**$[ZWA_2]^{2-}$** [b]
Asp	-12.7	-11.6	-2.3	-6.4
Glu	-14.4	-14.1	-1.2	-14.5
Cys	-15.6	-11.3	-6.0	-10.7
HCys	-15.4	-13.6	-6.5	-5.2

[a] Calculated with respect to the $[AA]^- + [Ch]^+$ dissociation.
[b] Calculated with respect to the $2[AA]^-$ dissociation.

We first consider the opposite charge ionic couples [Ch][AA] and [Ch][ZWA]. All the opposite-charge dimers are characterized by a strong H-bond that binds the hydroxyl to the carboxylate group. These ionic couples are rather stable for all AAs. The [Ch][ZWA] dimers have similar binding energies to their cation/anion counterparts, but, apart from $[Glu]^-$, these ionic couples are significantly

less stable. The [Ch][Glu] ZWA isomer, in fact, has an association energy which is competitive with its anionic form.

Moving to the like-charge dimers ($[AA_2]^{2-}$ and $[ZWA_2]^{2-}$), we find that both the $[Asp_2]^{2-}$ and $[Glu_2]^{2-}$ complexes are only slightly stable with respect to dissociation in their anionic forms. The two dimers can, however, bind much more strongly when they are found in their ZWA forms. These forms of the AAs form a type of "diamond" arrangement (see Figure 1) between two pairs of interacting protic groups which is seen to bind through a "salt-bridge" double H-bond that makes these conformations particularly stable with a binding energy which is comparable if not greater than the cation/anion one. The hydrogen bonding features observed in these structures, involves the positively charged amino group and the carboxylate group which shares both an intra- and inter-molecular interaction. The fact that the binding energy between pair of like-charge ions is comparable in size to the one of cation/anion pairs bears a huge influence on the properties of the bulk liquid and indicates that all those chemical processes which require a contact between anions, such as charge transfer, become likely to occur.

The two sulphur-containing AAs dimers (see figures 2 and 3) are found to be stable with respect to dissociation either in their plain anionic form and in the ZWA one. $[Cys]^-$ has a thiol group in its side chain which provides a possible proton donor group (in water –SH is a weak acid). The proton on this group is unstable and can transfer to another anion to produce a zwitterionic moiety. Inter and intra-molecular proton transfer has already been observed in molecular dynamic simulations of [Ch][Cys] [10] although, as we shall see more in detail below, proton transfer from the –SH moiety appears to represent only a sporadic event. The $[HCys]^-$ amino acid anion shares a similar structure to $[Cys]^-$ (difference of CH_2 in the alkyl chain) with the same hydrogen bonding interaction arising from the carboxylate and hydroxyl group on the cation. This makes both [Ch][Cys] and [Ch][HCys] systems where opposite charge aggregation is largely dominant with respect to like-charge clustering. We shall explore these findings in more detail in the next sections using the results of our MD simulations because such cooperative effects are crucial to the understanding of the bulk state of these compounds.

Although thermodynamics has shown that like-charge clustering of anions seems to represent a possible component of the bulk fluid (to a greater extent for [Glu] with respect to all others), proton transfer requires the cleavage of a rather stable O—H or S—H bond. In this respect, we remark that the different dielectric properties of the pure ionic liquid with respect to water makes the determination of the protonation/deprotonation sites based on well-known aqueous pKa values not entirely reliable. For this reason, we have tried to further characterize the proton transfer process by calculating the kinetic barriers to the isomerization reactions from the anionic dimer $[AA_2]^{2-}$ to the

zwitterionic one $[ZWA_2]^{2-}$. For $[Asp_2]^{2-}$ and $[Glu_2]^{2-}$ the determination of the transition state turned out impossible because these compounds do not present a simple (one step) mechanism of proton transfer from the acidic side chain to the amino group. The dynamics of this process is far more complex and stem naturally in the fluid only due to cooperative effects (as we shall show below). The barrier to isomerization reaction in the anionic dimer has been instead computed for $[Cys_2]^{2-}$ and $[HCys_2]^{2-}$ at the B3LYP-D3/6-311+G**/PCM. The isomerization from $[AA_2]^{2-}$ to $[ZWA_2]^{2-}$ takes place through a two-step mechanism that corresponds to the two protons moving from the –SH to the $–NH_2$ groups. For the $[Cys_2]^{2-}$ dimer, the enthalpy of both barriers is very low and turned out to be 0.2 and 0.9 kcal/mol for the first and second proton transfer respectively. The same data are 1.5 and 1.9 kcal/mol for $[HCys_2]^{2-}$. We conclude that, for both compounds, the proton transfer process has the possibility to occur rapidly even at low temperatures.

4. Study of the bulk phase

Due to the singly deprotonated nature of the AAs, and, given that the thermodynamics of proton migration is favourable (as shown in the previous section), in the bulk phase, we deal with a rather complex mixture of H-bond acceptors/donors: we have carboxylic/thiolic functions (–COOH/–SH) and ammonium ($–NH_3^+$) groups acting as donors while, at the same time, we have carboxylate/thiolate ($–COO^-$/$–S^-$) and amino ($–NH_2$) groups as acceptors. In addition, we also have the hydroxyl group on $[Ch]^+$ acting as an additional donor site. We will approach the analysis of the various molecular interactions by describing separately the anion-cation ones from those due to anion-anion pairs. We begin by examining the carboxylic AAs. In particular, we focus on the [Ch][Glu] system and we use the results of [Ch][Asp] as a reference, because the bulk properties of the two fluids are quite similar ([Glu] is the superior homologue of [Asp]).

Figure 4 shows the main source of interactions between cations and [Glu] anions. On $[Ch]^+$ we have one main interaction sites that is the hydroxyl group (–OH). The radial distribution functions (RDF) of the hydroxyl hydrogen on $[Ch]^+$ with different acceptor proton sites on $[Glu]^-$ is reported in different colors in the left panel of Figure 4: with the $–NH_2$ group (black line: H/N distance), with the $–COO^-$ group (red line: H/O distance) and with the –COOH one (green line). As one might expect, the most intense interaction of –OH group is with the $–COO^-$ group, where a strong H-bond is established assisted by the negative charge on the carboxylate oxygen. The weaker version of the same H-bond is present for NH_2, while is negligible for the available carboxylic terminals COOH. Despite the different abundance, if we stick to the geometry, we can assume that all three interactions are, in fact, H-bonds where the proton distance from the acceptor group (COO^-, NH_2 and COOH respectively) lies between 1.5-2.2 Å. Given these distances we can infer that proton transfer toward

the hydroxyl group of choline is not taking place at all. The contacts between the $(CH_3)_3N^+$ system of $[Ch]^+$ and the various protic/charged groups of $[Glu]^-$, are shown in the central panel of Figure 4, where we report the RDF between the positively charged N and the heteroatoms on $[Glu]^-$. These are less defined in terms of average inter-atomic distances with respect to the hydroxyl ones seen before and arise due mainly to long-range electrostatic and to molecular packing.
In the right panel of Figure 4, we have reported the RDF between the $[Ch]^+$ hydroxyl hydrogen, but for the $[Asp]^-$ AA. The situation is qualitatively similar to the [Ch][Glu] fluid, but the OH/NH_2 H-bonds are more abundant, a fact that is linked to the reduced structural flexibility of the $[Asp]^-$ AA. In $[Glu]^-$ we also observe a much reduced COOH/HO interaction with respect to $[Asp]^-$ because, as we shall see, most of the COOH protons have transferred to the amino group therefore leaving only very few carboxylate functional groups.

The interaction between two different anions is less intuitive and more difficult to rationalize. The driving force of anionic aggregation is the formation of multiple H-bonds that must overcome the natural repulsive interaction between the two $–COO^-$ groups on the two anions. We know from previous analysis [12] of other [Ch][AA] liquids that the average distance between the two negatively charged carboxylate on two different AAs is greater than 5-6 Å depending on the molecular size. Evidently, this distance is sufficient to decrease the electrostatic repulsion to the point in which H-bond can induce anion clustering, also helped by the relative high dielectric screening that further decreases electrostatic forces. In Figure 5 we report the RDFs between the protons initially residing on the COOH terminal of the AAs and the possible acceptor sites on the other AAs. The black line corresponds to a proton that interacts with the amino group and the red one to a proton that interacts with another carboxylate. The main peak of these radial distributions at around 1 Å, with a significant component below this value, indicates that the H-bond is very strong and that a certain degree of proton transfer has occurred from COOH to NH_2 or COO^- and that the proton now resides within the immediate neighbouring of the acceptor whether N or O. While the H—N radial distribution function (black line) shows essentially only one peak, the H-O one (red line) shows two peaks at short range the second being at 1.5 Å. The latter is obviously due to the presence of the second oxygen in the acceptor carboxylate. We conclude that the proton on the acidic side chain of $[Glu]^-$ can migrate easily onto the other anions while it does not migrate onto cations. We also see that proton transfer is taking place especially towards the NH_2 group as we can infer by considering the small size of the second peak in the H^+/N RDF (black line) at 1.7 Å that should represent the very small fraction of COOH that do not form an H-bond with amino groups. By looking at the molecular arrangements sampled by our dynamics we can also say that while the proton transfer toward the amino group is only seldom

reversible, that toward another carboxylate is reversible as one could easily expect for a resonant process.

The possibility of forming a neutral H-bond between two protonated COOH groups has been also investigated, but such interaction turned out to be negligible and only sporadic occurrences of such H-bond have been detected.

In the central panel of Figure 5 we report the RDFs between the oxygen atoms that are part of the carboxylic groups in various states of deprotonation. The first peak appears at 2.6 Å and identify the proton mediated H-bond. From the data we have gathered and presented in the left panel, we know that these O–O interactions are mediated by a charge assisted H-bond formed between two negatively charged carboxylate groups: $–COO^{\delta-}\cdots H^{+}\cdots{}^{\delta-}OOC–$.

If we compare the data collected for $[Glu]^-$ (left panel in Figure 5) with those for $[Asp]^-$ (right panel) we see that the two fluids behave in a similar way, with few important differences. We have said before that in $[Asp]^-$ fewer protons are migrating toward NH_2 during the simulations. This behaviour is consistent with the reduced stability of the ZWA dimers (with respect to $[Glu]^-$) that we showed in the ab-initio calculations and presented in Table 1. In particular, for $[Glu]^-$ the formation of $[ZWA_2]^{2-}$ dimers produces a more pronounced gain in association energy with respect to $[Asp]^-$ thereby favouring the proton transfer processes from the carboxylate to the amino groups. If we look at the radial distribution function of H^+/N in the right panel of Figure 5 (black line), we see that in $[Asp]^-$, there is an appreciable fraction of COOH that do not form an H-bond with amino groups as shown by the presence of a second peak at around 1.7 Å.

To have a pictorial representation of the bulk phase of [Ch][Glu], in Figure 6 we show the density surface representation obtained by a positional average of the cationic (blue) and anionic (red) positions along the production time: the aggregation of the anions (in red) is clearly shown by the spatial contiguity of the anionic domain, whereas the cations (in blue) are topologically isolated from each other and the blue density shows much fewer contacts. Most of these anionic clusters are found to be made by three anions connected together. An example arrangement of the three anions extracted from the simulations is further shown in Figure 6, below the density map. Out of three AA, the central one is a $[ZWA]^-$ with a positive NH_3^+ and two negative COO^-. The one on the right is a typical $[AA]^-$ with only one COO^-, while the one on the left is a doubly deprotonated anion.

Moving onto the sulphur based liquids, we report in Figure 7 the RDFs of the non-acidic choline –OH proton toward the various acceptors in the $[Cys]^-$ and $[HCys]^-$ AA. As for $[Glu]^-$ and $[Asp]^-$, the main interaction between anion and cation is the H-bond between the hydroxyl and the carboxylate (red lines). In the [Ch][Cys] system a substantial number of H-bonds exists also between the hydroxyl

and the NH_2 group of the AAs (black line). The interaction of the cation with the thiol group (green line) is clearly negligible for both $[Cys]^-$ and $[Hcys]^-$. All these H-bonds contacts have the maximum peak at distances well above 1 A thereby showing once again that, despite a strong H-bond, the proton on choline is not transferable.

Due to these short distances, we understand that the cationic and anionic species are found in proximity to each other although the thiol side chain functionality still plays a role in binding also the anions to each other. In order to explore the role of the thiol group in the [Ch][Cys] liquid, we report in Figure 8 the RDFs of its hydrogen with the various acceptor sites of the other anions. In the left panel of Figure 8, the interaction (black) at 1.8 Å corresponds to the thiol-amine H-bonds whereas the small (red) peak at 1.7 angstroms is the thiol-carboxylate interaction. Due to these distances, which are comparable to the ones we have found in the cation-anion H-bonding features, it is possible that inter-anionic hydrogen bonding is prominent in the [Ch][Cys] liquid and that anions are found to be relatively close to each other. Only very weak interactions (in green) are observed between two thiol groups.

Only a very limited proton mobility is observed in [Ch][Cys] as highlighted by the right panel of Figure 8 where the average distribution of S-H distances within the same AA molecule is reported. Such distribution is reported along with its volumetric running integral. Given that we have 56 ionic couples in the simulation box the limiting value of the integral measures the total number of S-bound protons. The distance distribution shows a shallow peaks at large distances that represent the fact that only a limited number of thiol protons (3 over 56) is no longer bound to sulphur, but has migrated onto the NH_2 group of the same molecule.

The same set of data discussed for $[Cys]^-$ is reported in Figure 9 for $[HCys]^-$. The latter behaves similarly with respect to $[Cys]^-$ especially for the NH_2—SH and COO^-—SH interactions. As before, the red line shows us that the SH is involved in rather strong H-bonds with the amino groups of other anions, but the H—N peak at 1.1 Å signify only a very limited chance of protons migrations onto the NH_2 groups. Also, it is important to note that during most the simulation the proton remains bonded exclusively to the thiol group (right panel, Figure 9).

5. Degree of (de)protonation on $[Asp]^-$ and $[Glu]^-$

Our previous analysis has pointed out a certain mobility of protons on the side chain of the examined systems: the result is that the possibility of transfer is greater when a carboxylic group is involved instead of a thiol group. However, the previous analysis does not allow us to quantify the degree of deprotonation of the side chain. To achieve this goal, we can use the RDFs reported in Figure 10. This figure shows the intramolecular COO—H distance and is reported along with its volumetric

integral. The integral of the first peak (at 1.1 Å) shows the average number of protons that remain attached to the COO group, the second peak at larger distances (1.4-2 Å) the protons that migrated onto a nearby NH_2/COO^- group. The third "peak", barely visible on the scale chosen, that we locate between 2.5 and 4 Å, represents those protons that have left the original COOH group and have moved in the liquid. In the [Glu][Ch] liquid only 15 protons remain attached to their original location onto the COOH group of the side chain. 9 protons have left their original location and have moved onto a nearby basic group (mostly NH_2). At least one proton has moved far away in the simulation cell. The situation for $[Asp]^-$ is very similar although our simulation cell contained less ionic couples and the total number of side-chain protons is 16.

Figure 11 shows the time elapsed proton migration (in percent) at a certain distance for several individual H atoms of the, initially, COO–H groups on the side chain of the $[Glu]^-$ AAs. We have highlighted only some of the significant bonds in the data (due to excessive overlap between the histograms). An example of two protons that remains localized on the side chain are represented by the black and purple histograms, where the proton is bound to COO for most of the time although the latter has a greater mobility than the former. The red and orange histograms represent the case of protons which are shared with an NH_2 group. The blue one, instead, shows the movements of a proton which has completely lost contact with the original COO^- group and has migrated into the liquid. In cyan we see a proton shared between two COO^- groups. The last case in green shows a proton that is hopping between its own COOH and an NH_2 group. It is possible to make similar considerations for the [Asp][Ch] system which is reported in the Supporting Information in Figure S7.

6. Conclusion

In this work, we have explored by means of computational methods, namely ab-initio calculations and molecular dynamic simulations, the structural complexity of a small subset of PILs. Our focus has been the formation of negatively charged zwitterionic species and the mechanisms of the ensuing proton transfer processes that take place in the bulk liquid. The systems under study are made up of a $[Ch]^+$ cation and a set of homologous AAs, specifically $[Asp]^-$, $[Glu]^-$, $[Cys]^-$ and $[HCys]^-$, all of which possess a secondary protic function on the side chain. These additional protic groups contribute to the complex hydrogen bonding network of the liquid impacting both its nanoscopic structure and its local charge distributions, hence affecting the bulk behaviours such as its frictional properties and conductivity (which might be enhanced by the presence of light charge carriers such as the migrating protons). The presence of a mobile proton on the side chain of the anion introduces complexity in these systems through two different transfer mechanisms: intra- or an inter-molecular proton transfer. In our MD simulations, we have clearly identified the existence of the unusual zwitterionic anions in

the bulk liquid which are a by-product of the presence of proton transfer processes. The relative stability of such zwitterionic species has been further confirmed by accurate ab-initio computations on the (continuum-solvated) isolated molecular structures.

While we have seen the formation of such zwitterionic transient chemical structures through sporadic single molecule tautomerization reactions, most of the times their formation is due to a proton transfer between two different anions. This instance requires that the anions come into contact due to cooperative hydrogen bonding which causes anionic species to cluster together overcoming their natural Coulombic repulsion. Interestingly we have also demonstrated that, isolated $[Glu_2]^{2-}$ and $[Asp_2]^{2-}$ dimers, once a sufficiently screening dielectric is present, overcome the electrostatic repulsion and form a dimer stabilized through multiple H-bonds which turns out to have a binding energy that is competitive with the cation-anion one. In contrast, the sulphur based AA ($[Cys]^-$ and $[HCys]^-$) show a reduced propensity in forming the $[AA_2]^{2-}$ dimers that we have found to be less stable that their oppositely charged counterpart [Ch][AA]. This result is further supported by the findings of our MD simulations where, in the case of the sulphur compounds, zwitterionic species were only a sporadic presence in the liquid and the ensuing proton transfer turned out to be only a minor process.

Acknowledgements

The financial support from "La Sapienza" (grant n. RM11715C7C86B2BE) is acknowledged. EB and AL gratefully acknowledge the computational support of CINECA (grant IscrC_COMPAA-2) and PRACE (grant n. 2016163881).

Supporting Information

Figure S1: Structural formulae of the aminoacids mentioned in this paper.

Figure S2-S6: Ab-initio optimized structures of all the aminoacid anionic.

Table S1: $\Delta H°$ of the intramolecular proton transfer

Table S2: Simulation data for all the systems.

References

[1] Welton, T. Room-temperature ionic liquids. solvents for synthesis and catalysis. *Chem. Rev*., **1999**, 99, 2071-2084.

[2] Hayes, R.; Warr, G.W.; Atkin, R. Structure and nanostructure in ionic liquids. *Chem.Rev.*, **2015**, 115, 6357-6426.

[3] Vekariya, R. A review of ionic liquids: Applications towards catalytic organic transformations. *J. Mol. Liq.*, **2017**, 227, 44-60.

[4] Hough, W.L.; Smiglak, M.; Rodrìguez, H.; Swatloski, R.P.; Spear, S.K.; Daly, D.Y.; Pernak, J.; Grisel, J.E.; Carliss, R.D.; Soutullo, M.D.; Davis, J.H., Jr.; Rogers, R.D. The third evolution of ionic liquids: active pharmaceutical ingredients. *New J. Chem*. **2007**, 31, 1429-1436.

[5] Doi, H.; Song, X.; Minofar, B.; Kanzaki, R.; Takamuku, T.; Umebayashi, Y. A new proton conductive liquid with no ions: pseudo-protic ionic liquids. *Chem. Eur. J*., **2013**, 19, 11522–11526.

[6] Stoimenovski, J.; Izgorodina, E.I.; MacFarlane, D.R. Ionicity and proton transfer in protic ionic liquids. *Phys. Chem. Chem. Phys*., **2010**, 12*,* 10341–10347.

[7] Bodo, E.; Mangialardo, S.; Capitani, F.; Gontrani, L.; Leonelli, F.; Postorino, P. Interaction of a long alkyl chain protic ionic liquid and water. *J. Chem. Phys.*, **2014,** 140, 204503/1–204503/10.

[8] Fumino, K.; Fossog, V.; Stange, P.; Paschek, D.; Hempelmann, R.; Ludwig, R. Controlling the subtle energy balance in protic ionic liquids: dispersion forces compete with hydrogen bonds. *Angew. Chem. Int. Ed.*, **2015,** 54, 2792–2795.

[9] Campetella, M.; Montagna, M.; Gontrani, L.; Scarpellini E.; Bodo, E.; Unexpected proton mobility in the bulk phase of cholinium-based ionic liquids. New insights from theoretical calculations. *Phys. Chem. Chem. Phys.* **2017,** 19, 11869-11880.

[10] Campetella, M.; Bodo, E.; Montagna, M.; De Santis, S.; Gontrani, L. Theoretical study of ionic liquids based on the cholinium cation. Ab initio simulations of their condensed phases. *J. Chem. Phys.*, **2016**, 144, 104504.

[11] Usula, M.; Matteoli, E.; Leonelli, F.: Mocci, F.; Marincola, F.C.; Gontrani, L.; Porcedda, S. Thermophysical properties of ammonium-based ionic liquid + N-methyl-2-pyrrolidone mixtures at 298.15K Fluid Phase Equil., 2014, 383, 49-54.

[12] Campetella, M.; Le Donne, A.; Daniele, M.; Gontrani, L.; Lupi, S.; Bodo, E.; Leonelli, F. Hydrogen bonding features in cholinium-based protic ionic liquids from molecular dynamics simulations. *J. Phys. Chem. B*, **2018**, 122, 2635-2645.

[13] Sawant, A.D.; Raut, D.G.; Darvatkar, N.B.; Salunkhe, M.M. Recent developments of task-specific ionic liquids in organic synthesis. *Green Chem. Lett. Rev.,* **2011**, 4, 41-54.

[14] Masci, G.; De Santis, S.; Casciotta, F.; Caminiti, R.; Scarpellini, E.; Campetella, M.; and Gontrani, L. Cholinium amino acid based ionic liquids: a new method of synthesis and physico-chemical characterization. *Phys. Chem. Chem. Phys.*, **2015,** 17, 20687−20698.

[15] Hou, X.D.; Liu, Q.P.; Smith, T. J.; Li, N.; Zong, M.H. Evaluation of toxicity and biodegradability of cholinium amino acids ionic liquids. *PLoS ONE*, **2013,** 8, 591451–7.

[16] Weaver, K.D.; Kim, H.J.; Sun, J.; MacFarlane, D.R.; Elliott, G.D. Cyto-toxicity and biocompatibility of a family of choline phosphate ionic liquids designed for pharmaceutical applications. *Green Chem*., **2012**, 12, 507–513.

[17] Nockemann, P.; Thijs, B.; Driesen, K.; Janssen, C.R.; Van Hecke, K.; Van Meervelt, L.; Kossmann, S.; Kirchner, B.; Binnemans, K.; Choline saccharinate and choline acesulfamate: ionic liquids with low toxicities. *J. Phys. Chem. B*, **2007,** 111, 5254–5263.

[18] Tao, G.H.; He, L.; Liu, W.S.; Xu, L.; Xiong, W.; Wang, T.; Kou, Y. Preparation, characterization and application of amino acid-based green ionic liquids. *Green Chem*., **2006,** 8, 639–646.

[19] Petkovic, M.; Ferguson, J.L.; Gunaratne, H.Q.N.; Ferreira, R.; Leitao, M.C.; Seddon, K.R.; Rebelo, L.P. N.; Pereira, C.S. Novel biocompatible cholinium-based ionic liquids-toxicity and biodegradability. *Green Chem*., **2012,** 12, 643–649.

[20] Plaquevent, J.-C.; Levillain, J.; Guillen, F.; Malhiac, C.; Gaumont, A.C. Ionic liquids: new targets and media for amino acid and peptide chemistry. *Chem. Reviews*, **2008**, 108, 5035–5060.

[21] Stoimenovski, J.; Dean, P.M.; Izgorodina, E.I.; MacFarlane, D.R. Protic pharmaceutical ionic liquids and solids: aspects of protonics. *Faraday Discuss*., **2012,** 154, 335−352.

[22] Belieres J.-F.; Angell, C.A. Protic ionic liquids: preparation, characterization, and proton free energy level representation. *J. Phys. Chem.* B, **2007**, 111, 4926-4937.

[23] Menne, S.; Pires, J.; Anouti, M.; Balducci, A. Protic ionic liquids as electrolytes for lithium-ion batteries. *Electrochem. Commun*., **2013**, 31, 39-41.

[24] Timperman, L.; Skowron, P.; Boisset, A.; Galiano, H.; Lemordant, D.; Frackowiak, E.; Beguin, F.; Anouti, M. Triethylammonium bis(tetrafluoromethylsulfonyl)amide protic ionic liquid as an electrolyte for electrical double-layer capacitors. *Phys. Chem. Chem. Phys*., **2012**, 14, 8199-8207.

[25] Eftekhari, A. Supercapacitors utilising ionic liquids. *Energy Storage Mater*. **2017**, 9, 47-69.

[26] Matsuoka, H.; Nakamoto, H.; Susan, M.A.B.H.; Watanabe, M. Brønsted acid base and poly base complexes as electrolytes for fuel cells under non-humidifying conditions. *Electrochim. Acta* **2005**, 50, 4015-4021.

[27] Ingnmey, J.; Gehrke, S.; Kirchner, B. How to Harvest Grotthuss Diffusion in protic ionic liquid electrolyte systems. *ChemSusChem*, **2018**, 11, 1900-1910.

[28] Benedetto, A.; Bodo, E.; Gontrani, L.; Ballone, P.; Caminiti, R. Aminoacid anions in organic ionic compounds. An ab-initio study of selected ion pairs, *J. Phys. Chem. B*, **2014**, 118, 2471.

[29] Le Donne, A; Bodo, E. Isomerization patterns and proton transfer in ionic liquids constituents as probed by ab-initio computation, *J. Mol. Liq.,* **2018**, 249, 1075-1082.

[30] Knorr, A; Stange, P.; Fumino, K.; Weinhold, F.; Ludwig, R. Spectroscopic evidence for clusters of like-charged ions in ionic liquids stabilized by cooperative hydrogen bonding. *ChemPhysChem*, **2016**, 17, 458-462.

[31] Knorr, A.; Fumino, K, Bonsa; A.-M.; Ludwig, R. Spectroscopic evidence of 'jumping and pecking' of cholinium and H-bond enhanced cation–cation interaction in ionic liquids. *Phys. Chem. Chem. Phys*., **2015**, *17*, 30978-30982.

[32] Strate, A.; Niemann, T.; Ludwig, R. Controlling the kinetic and thermodynamic stability of cationic clusters by the addition of molecules or counterions *Phys. Chem. Chem. Phys*., **2017**, *19*, 18854.

[33] Le Donne, A.; Adenusi, H.; Porcelli, F.; Bodo, E. Hydrogen bonding as a clustering agent in protic ionic liquids: like-charge vs opposite-charge dimer formation. *ACS Omega*, **2018**, 3, 10589–10600.

[34] Niemann, T.; Stange, P.; Strate, A.; Ludwig, R. Like-likes-like: cooperative hydrogen bonding overcomes coulomb repulsion in cationic clusters with net charges up to Q=+6e. *ChemPhysChem*, 2018, 19, 1691-1695.

[35] Niemann,T; Zaitsau, D.; Strate, A.; Villinger A.; Ludwig, R. Cationic clustering influences the phase behaviour of ionic liquid. *Sci. Rep.*, **2018**, 17505.

[36] Niemann, T.; Strate, A.; Ludwig, R.; Zeng, H.J; Menges, F.S.; Johnson, M.A. Spectroscopic evidence for an attractive cation–cation interaction in hydroxy-functionalized ionic liquids: A hydrogen–bonded chain-like trimer. *Angew. Chem. Int. Ed.*, **2018**, 57, 15364-15368.

[37] Ataman, E.; Isvoranu, C.; Andersen, JN.; Schnadt, J.; Schulte, K. Unconventional zwitterionic state of L-Cysteine. *J. Phys. Chem. Let.*, **2011**, 2*,* 1677-1681.

[38] Wojnarowska, Z.; Paluch, M. Recent progress on dielectric properties of protic ionic liquids. *J. Phys. Condens. Matter.*, **2015**, 27, 073202.

[39] Huang, M.-M.; Jiang, Y.; Sasisanker, P.; Driver, G.W.; Weingartner, H. Static relative dielectric permittivities of ionic liquids at 25°C. *J. Chem. Eng. Data*, **2011**, 56, 1494–1499.

[40] Grimme, S.; Antony, J.; Ehrlich, S.; Krieg, H. A consistent and accurate ab initio parameterization of density functional dispersion correction (DFT-D) for the 94 elements H-Pu. *J. Chem. Phys.*, **2010**, 132, 154104.

[41] Frisch, M.J.; Trucks, G.W.; Schlegel, H.B.; Scuseria, G.E.; Robb, M.A.; Cheeseman J.R.; Scalmani, G.; Barone, V.; Petersson, G.A.; Nakatsuji, H.; et al. *Gaussian 16*, revision B.01; Gaussian, Inc.: Wallingford, CT, **2016**.

[42] Hutter, J.; Alavi, A.; Deutsch, T.; Bernasconi, M.; Goedecker, S.; Marx, D.; Tuckerman, M.; Parrinello, M. CPMD version 3.9.1; IBM Research Division, IBM Corp and Max Planck Institute Stuttgart, **2004**.

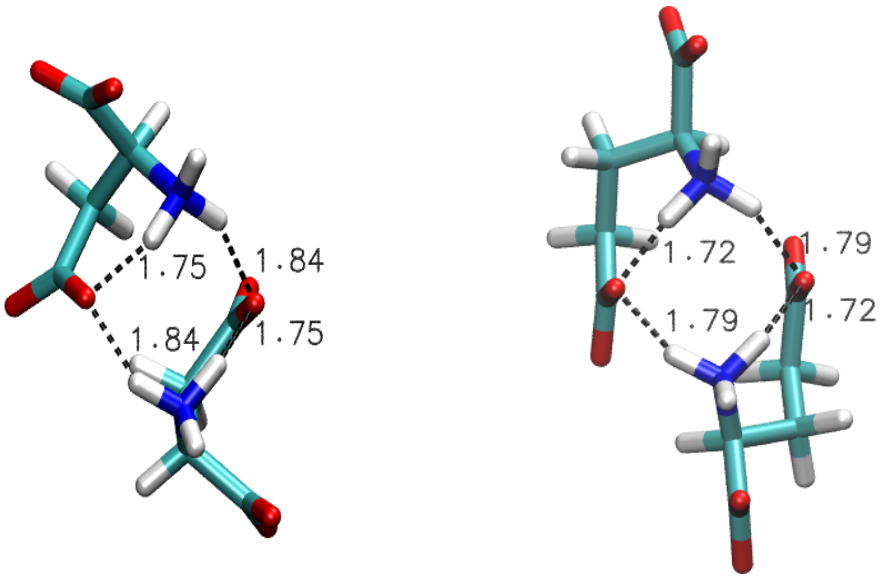

Figure 1: Optimized structure at the D3-B3LYP/PCM level for $[Asp_2]^{2-}$ (left) and $[Glu_2]^{2-}$ (right) ZWA/ZWA dimer. Acceptor donor distances in H-bonds are also shown.

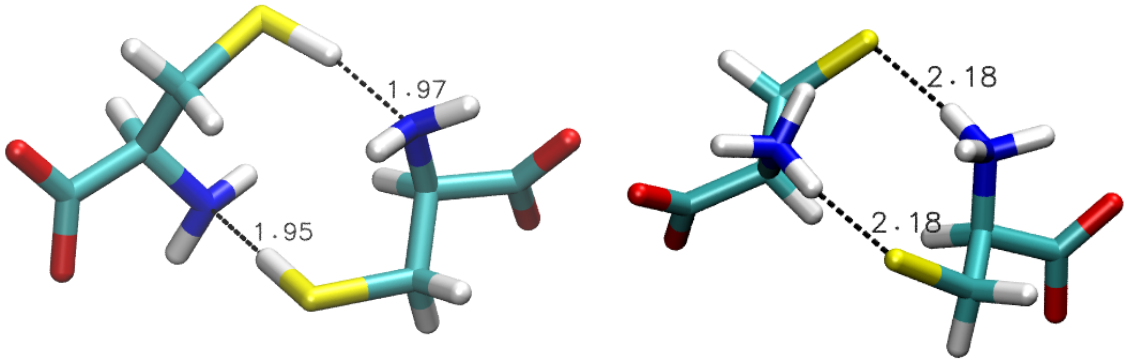

Figure 2: Optimized structures at the D3-B3LYP/PCM level for $[Cys_2]^{2-}$ anion/anion (left) and ZWA/ZWA (right) dimers. Acceptor donor distances in H-bonds are also shown.

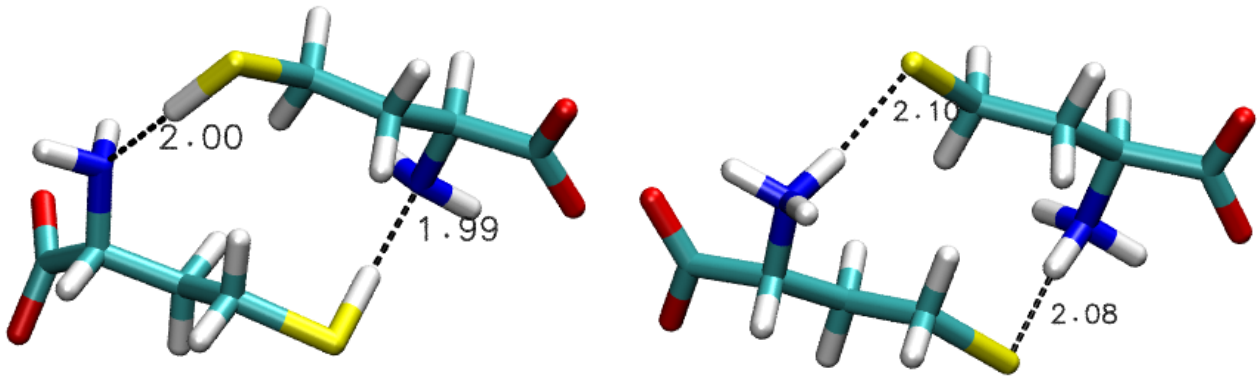

Figure 3: Optimized structures at the D3-B3LYP/PCM level for $[HCys_2]^{2-}$ anion/anion (left) and ZWA/ZWA (right) dimers. Acceptor donor distances in H-bonds are also shown.

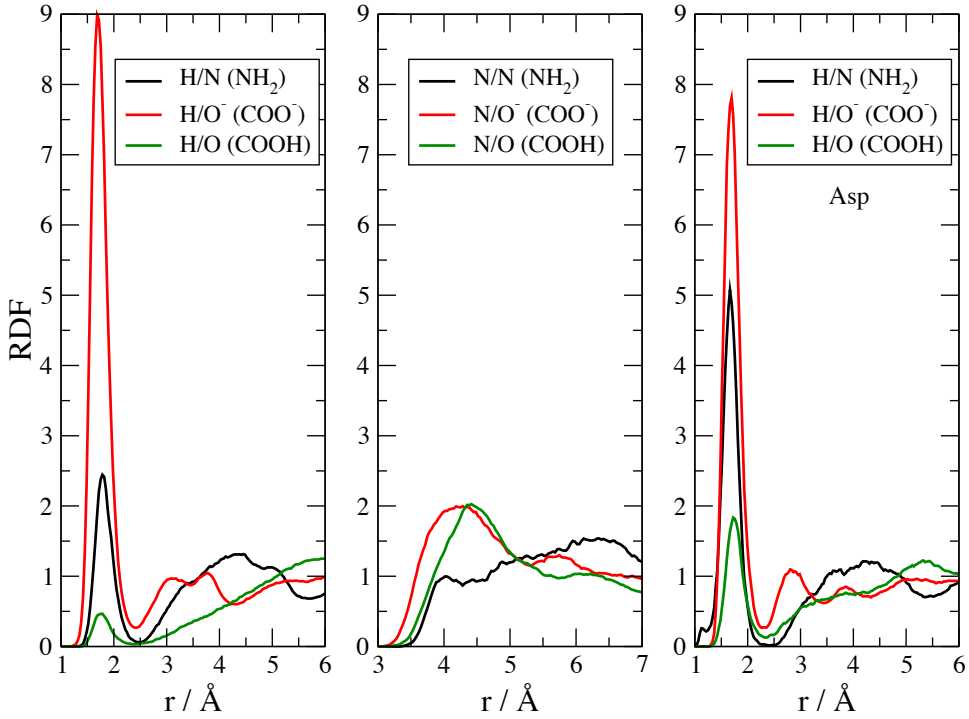

Figure 4: RDF between cation and anions: the left panel presents the RDF between the hydrogen of the hydroxyl on $[Ch]^+$ and the nitrogen of the amino group (black line), the oxygen of the carboxylate group (red line) and that of the carboxylic group (green line) of the $[Glu]^-$ anion. Central panel shows the RDF between the quaternary N of $[Ch]^+$ and interactions with the same AA functional groups. The right panel contain the same data as the left one, but for the [Ch][Asp] fluid.

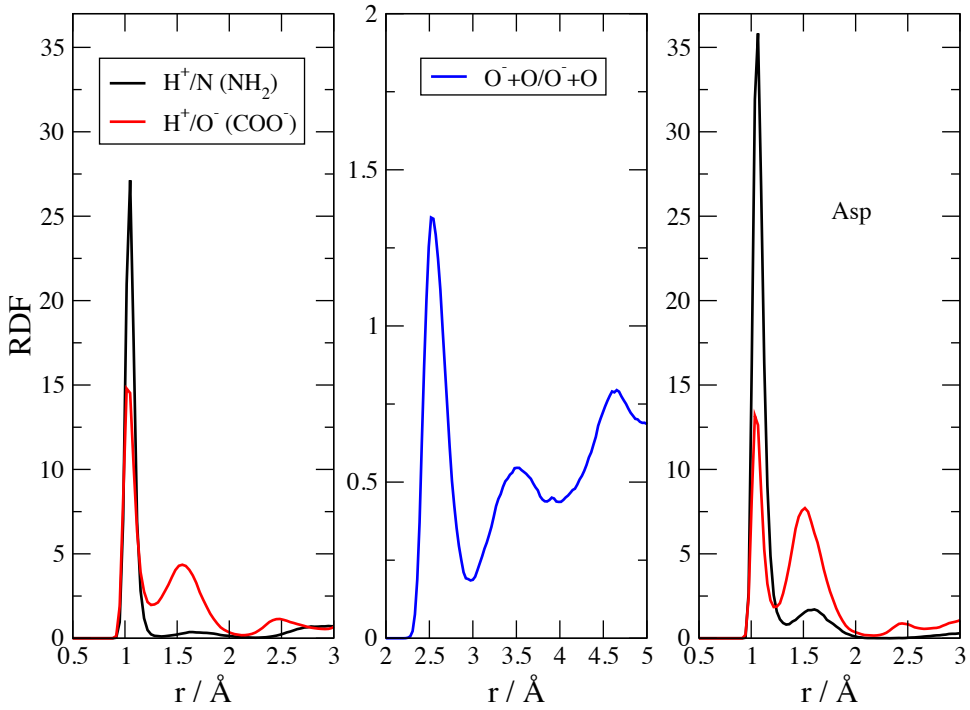

Figure 5: Inter-anionic RDF between anions: left panel shows the radial distribution for the proton (H) of the carboxylic groups of $[Glu]^-$ to the amino group (black) and to the carboxyl/carboxylate group (red). In the central panel we show the radial distribution function between all carboxylic oxygen atoms. The right panel contain the same data as the left one, but for the [Ch][Asp] fluid.

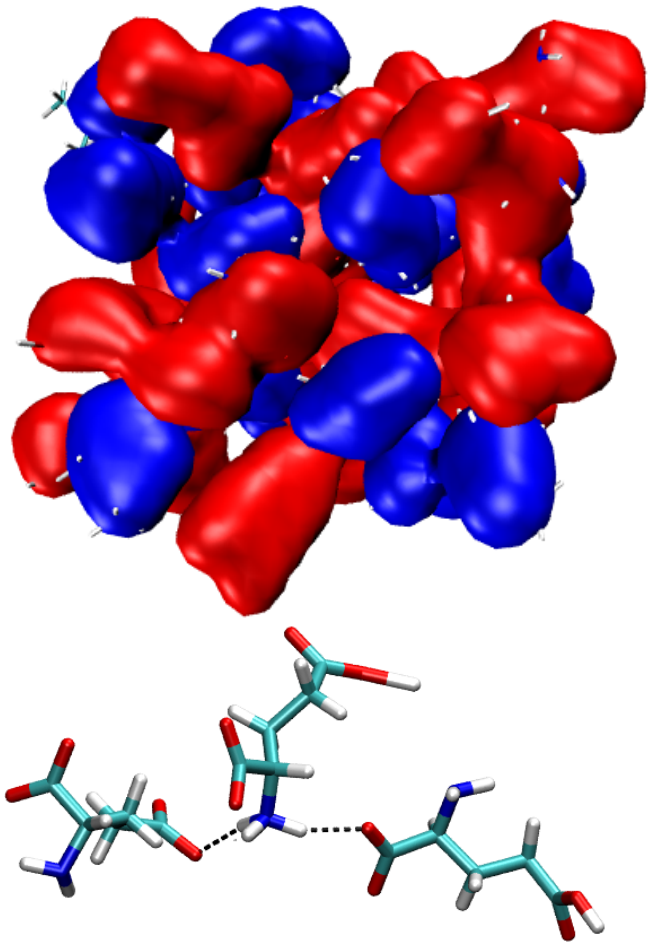

Figure 6: (Top) Volumetric map of the density surface of ionic liquid [Ch][Glu] calculated as positional average of the AIMD trajectory: cation density in blue, anion density in red. (Bottom) An example of the complex arrangement inside [Ch][Glu] IL from a snapshot: the $[Glu]^{2-}$ on left has protonated the amino group of the $[ZWA]^{-}$ at the centre whose NH_3^{+} group is interacting with two different carboxylate groups; the side chain of the $[Glu]^{-}$ at centre is sharing its proton with another anion which is not displayed.

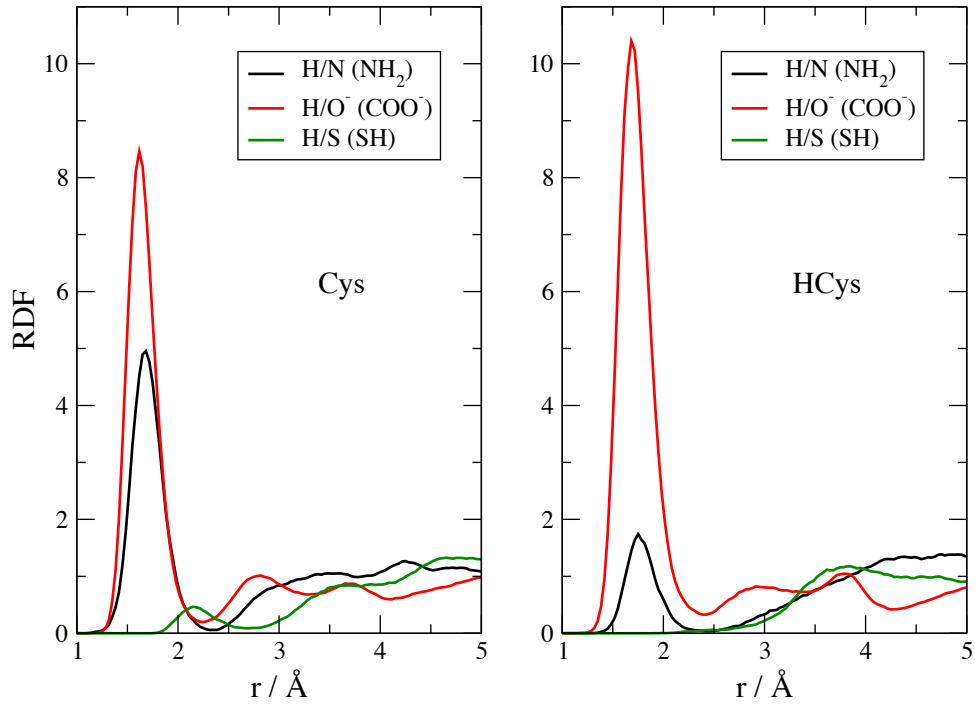

Figure 7: RDF between cation and anion of [Ch][Cys] (left) and [Ch][HCys] (right) focused on the distribution function of the H atom of the hydroxyl group of the choline: in black with the nitrogen of the anion amino group, in red with the carboxylate and in green with the thiol.

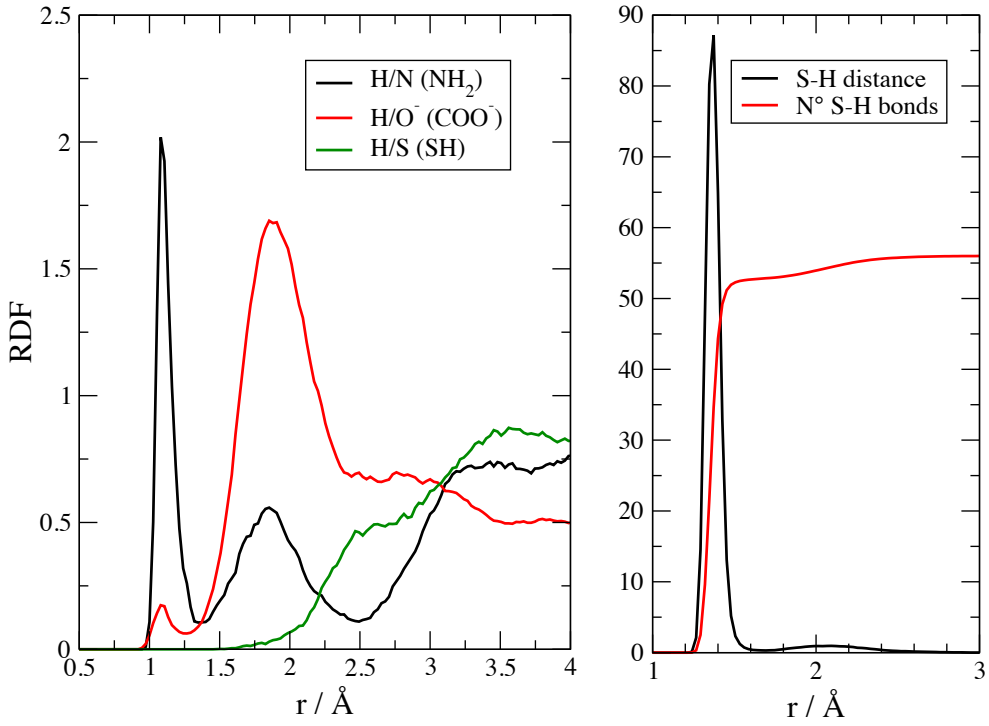

Figure 8: Left, inter-anionic RDF of $[Cys]^-$ focused on the hydrogen of the thiol group. Black line: with the amine group (S–H···NH_2). Red line: with the carboxylate group (S–H···O^-) and the distance (green) between this hydrogen and another thiol group (S–H···SH). Right, intra-molecular S–H RDF of $[Cys]^-$ and its cumulative volumetric integral.

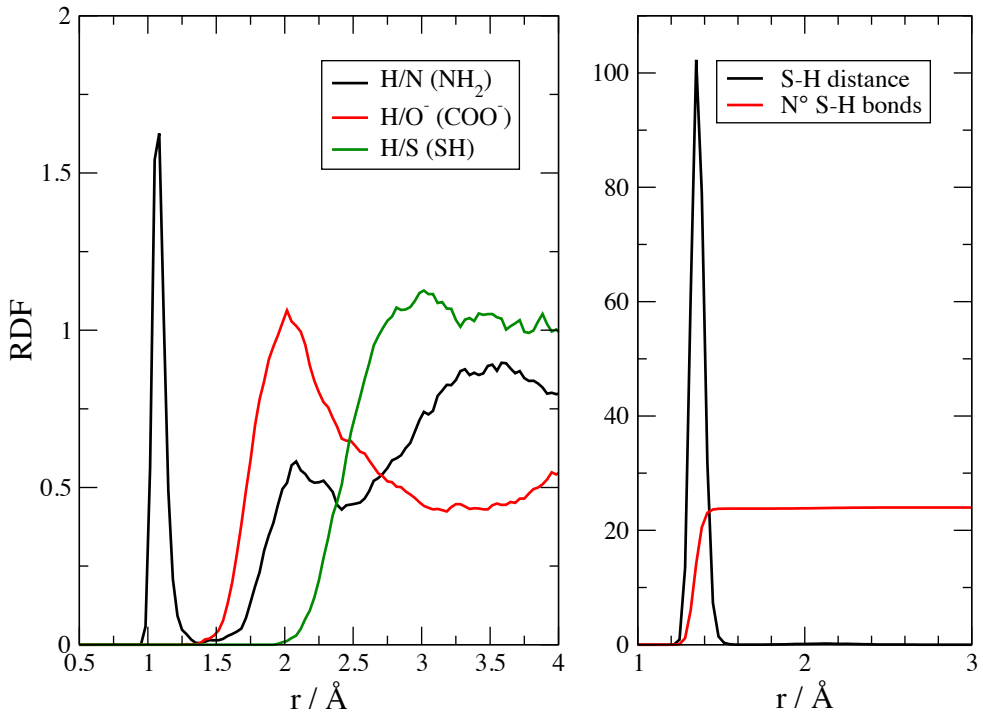

Figure 9: Left, inter-anionic RDF of $[HCys]^-$ focused on the hydrogen of the thiol group. Black line: with the amine group (S–H···NH_2). Red line: with the carboxylate group (S–H···O^-) and the distance (green) between this hydrogen and another thiol group (S–H···SH). Right, intra-molecular S–H RDF of $[HCys]^-$ and its cumulative volumetric integral.

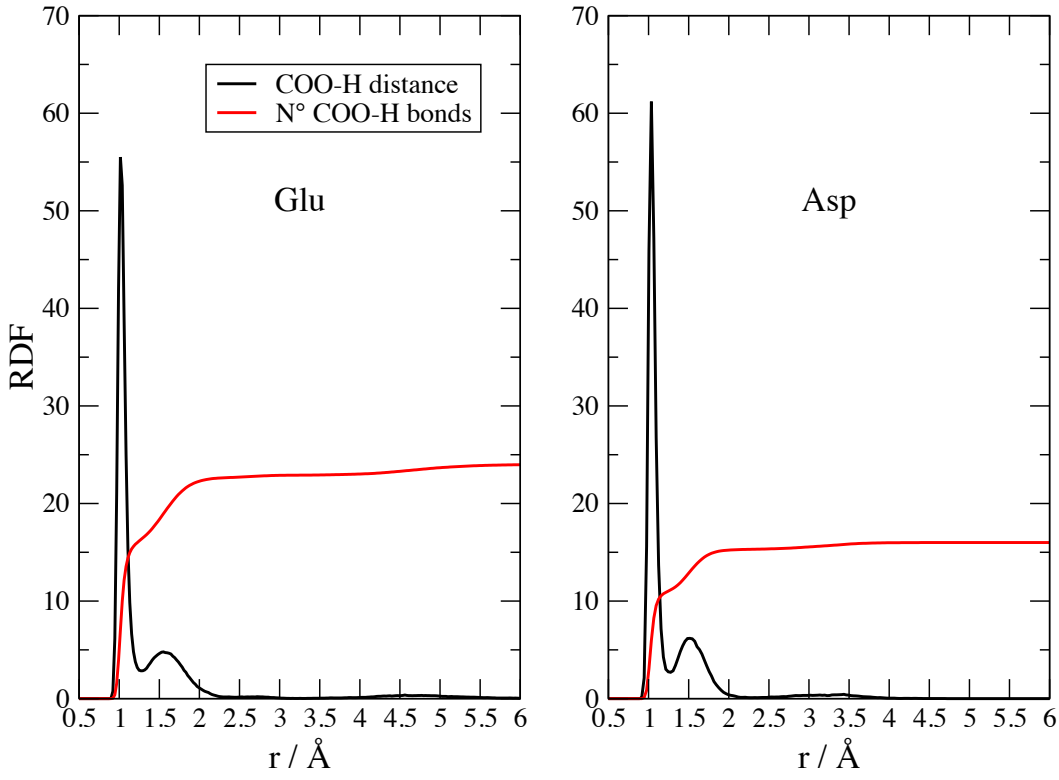

Figure 10: Intramolecular RDF of the COO—H distances ion $[Asp]^-$ (right) and $[Glu]^-$ (left). In the simulation cells there are 24 COOH protons in $[Glu]^-$ and 16 in $[Asp]^-$.

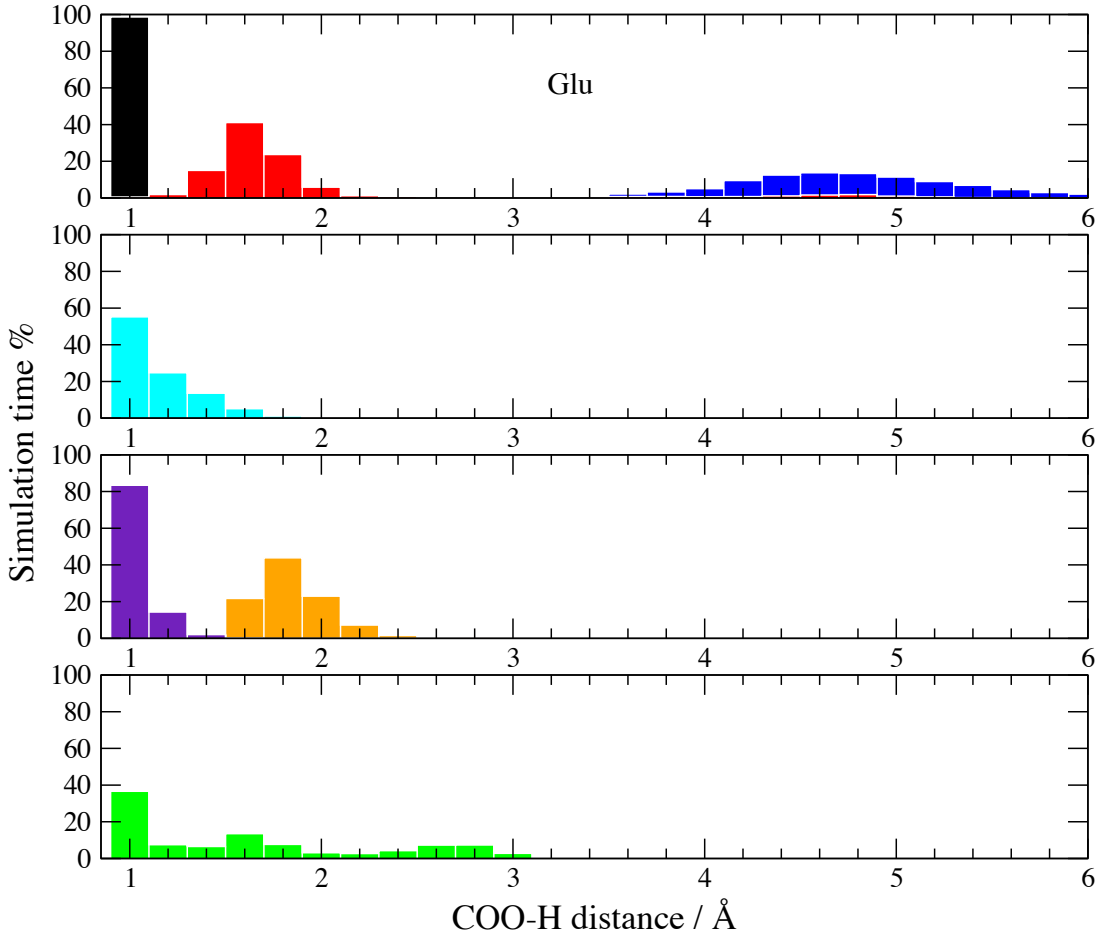

Figure 11: Histograms displaying the time elapsed proton migration (in percent) at a certain distance for the H atom of COO–H groups. See text for details.

TOC Graphic